Advanced High-Thrust Colloid Sources

M. N. HUBERMAN*
TRW Systems Group, Redondo Beach, Calif.
AND
S. G. ROSEN†
Edwards Air Force Base, Edwards, Calif.

This paper describes recent advances in the development of high-thrust tubular colloid sources for satellite applications. Single emitter technology has advanced to the point where steady reliable performance has been demonstrated at greater than 111 μN (25 μlb) per unit, 75% time-of-flight efficiency, and 1300 sec specific impulse for periods on the order of 100 hr. The most significant findings were the importance of orienting the emitter vertically in order to equalize gravitational effects around the emitter rim, the need to enlarge the extractor aperture, and the development of special tooling techniques for manufacturing emitters. A four-source module was subjected to extensive performance testing in addition to runs of 100 hr and 360 hr. Long-term steady performance was demonstrated at several levels up to 547 μN at 75% time-of-flight efficiency and 1325 sec specific impulse. The ability to neutralize the beam without interfering with thruster performance was also demonstrated. Beam probe measurements showed that 90% of the beam was contained within a 15° half angle. The thruster's ability to provide constant performance to within ±3% was also demonstrated. During short-term testing at high-feed pressures, the thruster produced 1339 μN at 70% efficiency and 1029 sec specific impulse.

Introduction

THE main purpose of the work described here was to continue the development of high-thrust colloid sources for satellite propulsion applications. Particular emphasis was placed on improving thruster efficiency and demonstrating reliable performance up to the 445 μN (100 μlb) range.‡ The major conclusions of the program were that large diameter tubular sources can produce more than ten times the thrust of a needle and can provide long-term stable operation at 75% efficiency and 1300 sec specific impulse. The fact that only one-tenth as many emitters are required for a given thrust level, results in increased reliability, smaller thruster size and weight, decreased mechanical complexity, and reduced manufacturing and testing costs. The reliability benefits can be envisioned in several ways. For example, if we assume that a single high-thrust source has the same failure rate as a single needle, then the failure probability for a complete thruster will be decreased by a factor of 10; i.e., an additional 9 will be added to the thruster reliability number.

General Approach

The basic thruster configuration is shown in Fig. 1. The main features of the emitter are a flow impedance tube for mass flow control, the emitter tip, which is designed to provide the proper emission characteristics, and an external shank to provide good mechanical and thermal coupling to the module base. The emitter is positioned within three deflector electrodes which, in turn, are centered in a $\frac{1}{2}$-in. extractor aperture. As their name implies, the deflector electrodes can be used to vector the colloid beam electrically. They also allow the extraction field strength to be modified independently of the total emitter accelerating voltage. Another function of the deflector electrodes

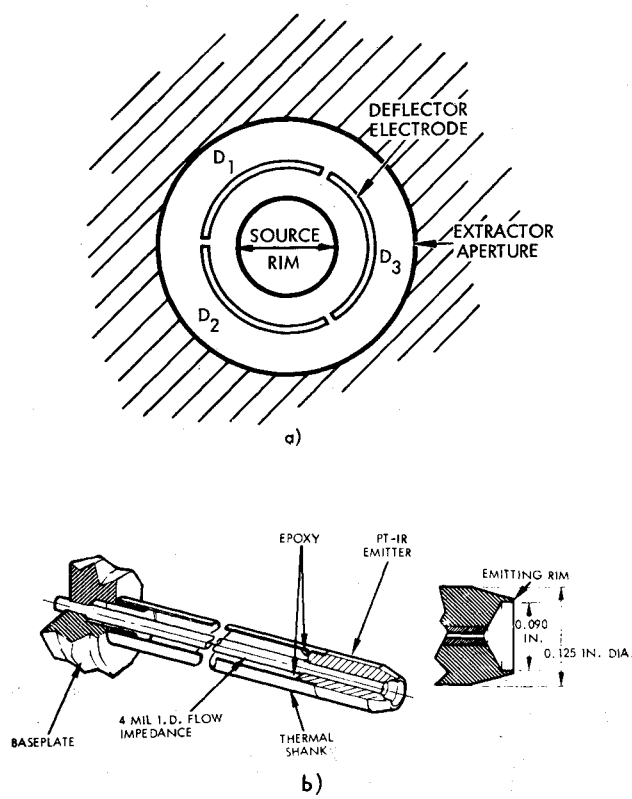

Fig. 1 High thrust source configuration. a) Electrode geometry; b) Emitter schematic.

Received October 29, 1973; presented as Paper 73-1075 at the AIAA 10th Electric Propulsion Conference, Lake Tahoe, Nev., October 31–November 2, 1973; revision received March 4, 1974.

Index category: Electric and Advanced Space Propulsion.

* Head, Colloid Propulsion Section, Product Technology Laboratory, Applied Technology Division.

† Capt. U.S. Air Force; also Project Engineer, Rocket Propulsion Laboratory.

‡ Unless otherwise stated, all results presented in this paper are based on time-of-flight measurements of the droplet velocity distribution within the beam. The velocity distributions are obtained by instantaneously switching the thruster off by shorting it to ground and then observing the time decay of the thruster current to a collector positioned on the order of 1 m downstream. These measurements are used to calculate thrust, specific impulse, charge-to-mass ratios, mass flow, and thruster efficiency. The efficiency in this case is defined as $T^2/2\dot{M}P$ where T and $\dot{M}$ are, respectively, the thrust and mass flow resulting from the time-of-flight calculations, and P is the product of the applied needle voltage times the current supplied to the thruster. The time-of-flight calculations neglect the effects of beam spread, an approximate 400-v loss in the spraying process, and the presence of neutral particles in the beam.

Table 1 Tool formed emitter run summary (most significant runs only)

Emitter no.	Extractor aperture	Orientation	Results
TM1	½ in.	Horizontal	Thrust 89–222 μN I_{sp} < 1200 sec usually Efficiency 60–65%
TM1	⅜ in.	Horizontal	Essentially the same as above Efficiency slightly lower Vertical probe showed off-set to bottom
TM1	½ in.	Horizontal	Deflector and extractor 0.010 in. forward Essentially same performance
TM2	½ in.	Vertical	77%, 1350 sec, 138 μN 74%, 1450 sec, 178 μN
TM3	½ in.	Vertical	Same as above 100 hr test at 76.6%, 159 μN, 1382 sec Best end point value: 78%, 1458 sec, 173 μN
TM1 (Deeper well)	½ in.	Vertical	80%, 1300 sec, 118 μN 76%, 1500 sec, 124 μN
TM1 (Deeper well)	½ in.	Vertical	Essentially same as performance above

is to modify the field in front of the thruster in such a way as to make it difficult for returning ions to strike the extractor in the region immediately adjacent to the extractor aperture, where they could create secondary electrons which have a high probability of bombarding the emitter tip. Furthermore, the deflector electrodes also provide line-of-sight mechanical shielding between the emitter and extractor.

The major program goal was to increase thruster efficiency without degrading operational stability or other performance parameters such as thrust or specific impulse. The interrelationship between the performance parameters can best be seen from the fact that the specific impulse is proportional to the square root of the product of the net accelerating voltage, the average charge-to-mass ratio, and the specific charge distribution efficiency. The first two variables can be increased by raising the total source voltage while holding all other control parameters constant since this increases the extraction field strength and the average charge-to-mass ratio. However, raising the voltage in this manner can increase the thruster exhaust's ion content, thus lowering the beam efficiency. Also, past observations have often indicated that higher efficiencies can be achieved at lower charge-to-mass ratios. For a given accelerating voltage this would result in lower specific impulse. For these reasons it is desirable to decouple the total thruster voltage from the extraction field strength so that these quantities can be adjusted independently in order to insure that thruster performance is fully optimized.

The deflector electrodes satisfy the above mentioned requirement by allowing the extraction field to be modified so as to require a higher total accelerating voltage for a given field strength and charge-to-mass ratio. Thus, a major experimental approach was to work at higher deflector voltages in order to obtain lower charge-to-mass ratio and higher efficiency while maintaining high specific impulse.

In addition to the previous considerations which would apply to any specific thruster geometrical configuration, variations in geometry were also investigated as a means of improving performance. There are several ways in which the thruster geometry impacts on performance. For example, the emitter rim thickness is one of the factors which determine the field strength and uniformity in the vicinity of the emitting region. Similarly, the deflector-to-emitter spacing, the extractor aperture diameter, and the relative heights of the deflector, emitter, and extractor all influence the trajectories of returning secondary particles, the probability of electron emission from thruster surfaces, beam focusing, collision probabilities and energies within the thruster exhaust, and field strength and uniformity at the emitter tip. Furthermore, the emitter tip interior geometry and surface condition affect the propellant depth and surface configuration in the vicinity of the emission region. All the foregoing effects are interrelated and no adequate theoretical treatment exists. For this reason, variations in these parameters were experimentally investigated to determine if performance improvements could be attained relative to the baseline design. The major finding was that widening the extractor aperture extended the range of stable high-voltage performance, thus allowing lower charge-to-mass operation while still maintaining adequately high specific impulse.

Changing to a vertical thruster orientation in order to eliminate meniscus nonuniformities caused by the gravitational effects within the emitter also produced a major performance gain. Another significant improvement was the development of an emitter forming tool which provided two major advantages: 1) emitter-to-emitter mechanical reproducibility, and 2) complete rim uniformity around the entire emitter perimeter. The latter feature is particularly crucial because there is an optimum combination of field strength, field direction, and mass flow for achieving stable high-performance operation. Variations in the detailed emitter rim geometry around the perimeter will cause corresponding variations in the above mentioned parameters, resulting in off-optimum local operating conditions. The rim forming tool provided a simple solution to this problem, and is discussed later.

Steady reliable performance for a single emitter was demonstrated at greater than 111 μN (25 μlb) per unit, 75% efficiency and 1300 sec specific impulse for periods on the order of 100 hr. This was achieved after performing an extensive test program on a wide variety of thruster configurations.

Table 1 is a summary of the most significant runs with tool formed emitters and a comparison of the horizontal and vertical operation. The main conclusions drawn from these tests were 1) for a given orientation the performance was reproducible from one emitter to the next, 2) tool-formed emitters operated very smoothly at fairly high performance levels, and 3) vertical operation resulted in higher stable operating levels, especially with regard to thruster efficiency. A single-emitter, 100-hr life test was run prior to instituting the multisource array work. Tables 2 and 3 are summaries of the average performance and control parameters over the entire test.

Thrust Vectoring

The ability to thrust vector a colloid engine increases its applicability for flight applications by allowing it to perform

Table 2 100-hr life test summary (run 7208-06) control parameters

Emitter	No. 3
Extractor aperture	½ in.
Orientation	Vertical
Source voltage	19 kv
Deflector voltage	15 kv
Extractor voltage	−2 kv
Feed pressure	5 in. Hg

Table 3 100-hr life test summary (run 7208-06) performance parameters

Source current	74 μa
Extractor current	0.2 μa
Deflector current	0 μa
Efficiency	76.6%
Thrust	159 μN
Specific impulse	1382 sec
Mass flow	11.72 μg/sec
Charge-to-mass ratio	6370 c/kg

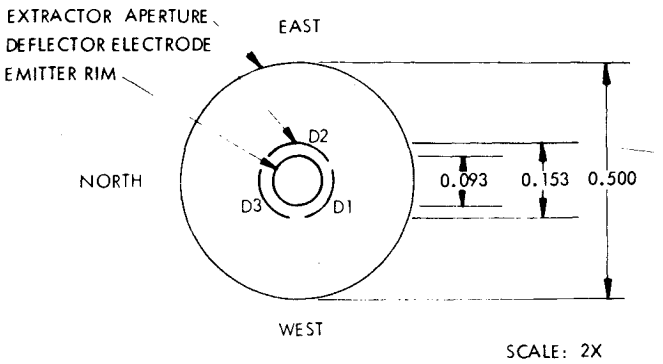

Fig. 2 Schematic—vector electrode arrangement (dimensions, in inches).

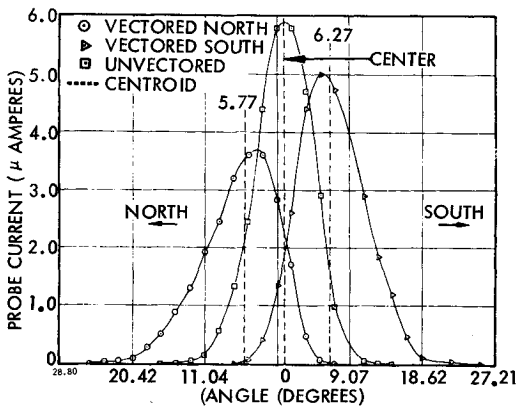

Fig. 3 North-south vectoring response, performance parameters are shown in Table 4.

thrust misalignment corrections and center-of-mass shift compensation in addition to allowing a single thruster to perform multiple spacecraft functions such as stationkeeping and attitude control. Electrostatic vectoring is a particularly appealing concept in that it eliminates the moving mechanical parts required by other vectoring techniques.

The electrostatic vectoring of various colloid thrusters has been demonstrated many times in the past,[1-5] but whenever the thruster performance level or design geometry is changed it can be expected that there will be a change in the vectoring response of an electrostatic system. For this reason several runs were made to check the thrust vectoring response of a single source in its present developmental state.

Table 4 Performance data for Fig. 3 (source voltage = 18.2 kv, extractor voltage = −2 kv, feed pressure = 5 in. Hg)

V_{D1} (kv)	V_{D2} (kv)	V_{D3} (kv)	(%)	I_{sp} (sec)	Thrust (μN)	Mode
14	14	14	76.9	1405	129	Unvectored
20	14	7.5	65.8	1302	113	Centroid deflected north 5.8°
7.4	14	20	65.8	1237	122	Centroid deflected south 6.3°

As previously mentioned, three deflector electrodes are used to provide an x-y vectoring capability. Figure 2 shows their relative orientation. There are several reasons for using three electrodes instead of the more intuitively acceptable four electrode array which is easier to visualize in terms of separate x and y vectoring control. The advantages of having three electrodes are as follows: 1) a three-fold vectoring symmetry considerably simplifies the underlying electrode support structure for a hexagonally close packed source array; 2) one less power supply is required than for a four-fold system; and 3) use of a conventional four-fold x-y vectoring system would probably require a square packing geometry for the source which would result in a lower thrust density than for a hexagonal array. A possible advantage of the four-electrode system is that it may be easier to program in a given off-axis vectoring angle.

During the vectoring runs, it was easy to demonstrate that the thrust vector direction could be significantly influenced by the application of deflecting voltages. The beam profile could be visually discerned by the fluorescent pattern on the collector and the motion of the beam pattern in response to application of deflecting voltages was dramatic corroboration of the thruster vectorability.

The thruster was pointed straight down and the beam profile was scanned across its midplane by two 2 × 5 cm probes. The east-west probe scanned through a plane 68.6 cm downstream of the thruster. The north-south probe scanned through a plane 71.8 cm downstream of the thruster.

Figure 3 and Table 4 summarize the results from a north-south vectoring scan. It can be seen from Table 4 that the north-south vectoring was obtained by varying the biases on deflectors 1 and 3 relative to each other while holding deflector 2 constant. In this case, deflections of 5.8° and 6.3° were obtained at the cost of some reduction in efficiency and specific impulse.

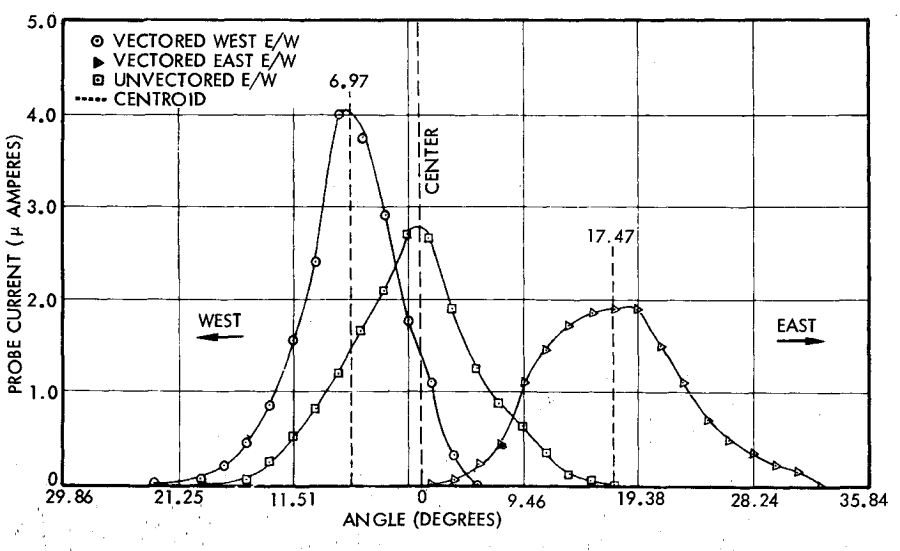

Fig. 4 East-west probe of the beam during east-west vectoring.

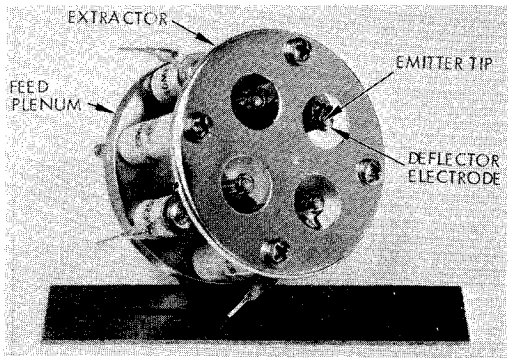

Fig. 5 Four-source array.

Table 5 Performance dependence on deflector voltage after 115 hr (source voltage = 18 kv, extractor voltage = −5 kv, feed pressure = 13 in. Hg, temperature = 25°C)

Deflection voltage (kv)	Efficiency (%)	Specific impulse (sec)	Thrust μN (μlb)
16.6	76.7	1025	438 (98.5)
16.4	76.0	1043	516 (113.7)
16.2	77.2	1084	604 (135.7)
16.0	76.6	1123	665 (149.4)
15.8	76.6	1155	704 (158.3)
15.6	75.9	1184	754 (169.5)
15.4	75.4	1226	792 (178.0)
15.2	73.4	1216	845 (190.0)

An east-west probe of the beam showed a slight shift to the west during both north and south vectoring. This effect would be less likely to occur with a four-electrode system that would be totally symmetric in the east-west direction during north-south vectoring.

Figure 4 shows the east-west vectoring data obtained by maintaining equal voltages on D_1 and D_3 and by varying the two relative to D_2. Thus, the deflector voltages were 1) undeflected $V_{D_1} = V_{D_2} = V_{D_3} = 14$ kv, 2) deflected west $V_{D_1} = V_{D_3} = 8.7$ kv, $V_{D_2} = 22$ kv, 3) deflected east $V_{D_1} = V_{D_3} = 22$ kv, $V_{D_2} = 2.5$ kv. The net deflection angles for the centroid were 7° east and 17.5° west.

Multisource Arrays

Three-source and four-source arrays with frontal areas just under 4 sq in. were fabricated in order to investigate the properties of thruster operation at approximately 445 μN levels.

The individual emitter impedances varied less than ±2% from the mean impedance value. Instead of three vector electrodes, each emitter had one continuous shield electrode surrounding its tip. This allowed a considerable reduction in structural complexity over that which would be required for complete sets of vectoring electrodes. To maintain ease of alignment, each shield electrode was mounted on its own individual support structure. Two examples of high performance at 75% efficiency for the three-emitter source are: a specific impulse of 1470 sec at a thrust of 311 μN, and, a specific impulse of 1340 sec at a thrust of 414 μN. In general, it was possible to obtain thrust in excess of 445 μN (100 μlb), specific impulse in excess of 1500 sec, and thrust efficiency greater than 75%, all with stable, smooth operation. However, it was not possible to achieve all three goals simultaneously. This was mainly because the thruster had to be pushed hard to achieve a total of 445 μN for three emitters. Consequently a decision was made to build the four-source-array for the 445 μN thrust level.

The four-source array is shown in Fig. 5. For convenience, the four sources are arranged in a square pattern $\frac{3}{4}$ in. on a side with $\frac{1}{2}$-in.-diam extractor apertures. The over-all thruster diameter is 2.25 in., resulting in a frontal area just under 4 sq in. Thruster temperature is monitored by the usual technique of placing a thermistor probe in the module base plate. Thruster temperature readings are then used to regulate a radiant heater which surrounds the thruster.

Two longer duration tests of 360 hr and 100 hr were run with the array. The main purpose of the first run was to conduct a preliminary test of the thruster's ability to perform over durations of 100 hr at various performance levels. The total test duration was 360 hr which included, in addition to long runs at various performance levels, demonstration of neutralized performance and profile mapping of the angular beam spread.

Figure 6 shows the total performance time history. It can be seen that there were three main segments to the test, each of the order of 100 hr or greater duration. The time-of-flight efficiency was greater than 75% for all three periods. For the first period the thrust averaged slightly over 445 μN and the average specific impulse was approximately 1025 sec. This was achieved at 18 kv source voltage, 16.6 kv deflector voltage, −5 kv

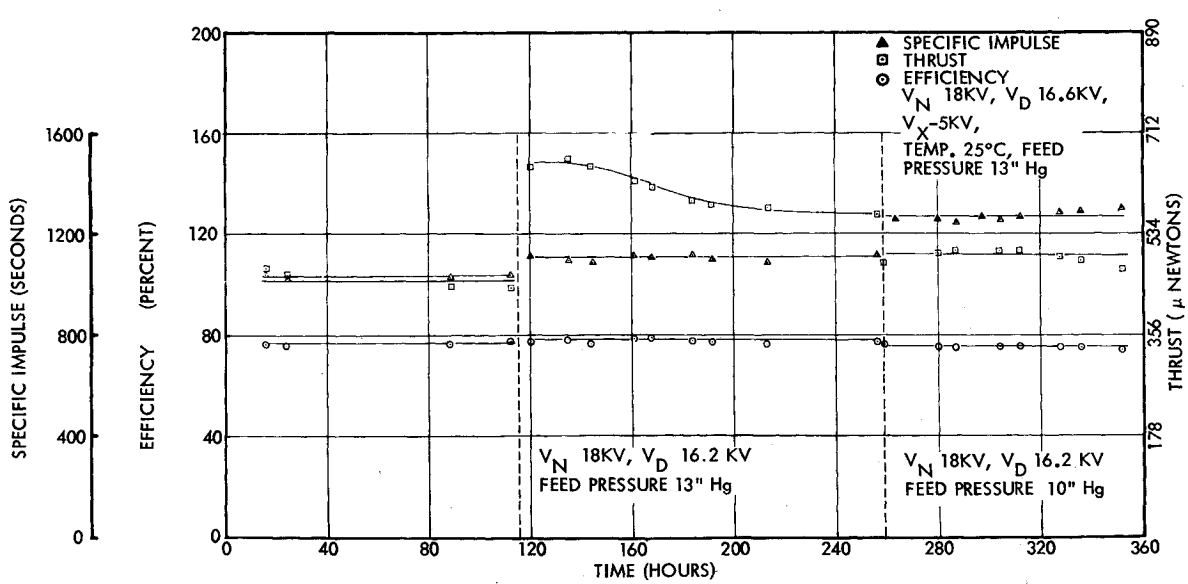

Fig. 6 Performance time history—360-hr test.

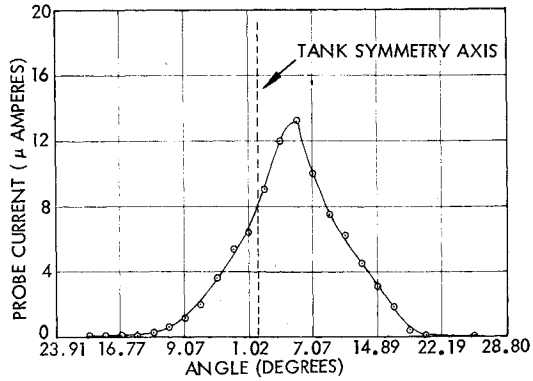

Fig. 7 North-south beam profile during last third of 360-hr test.

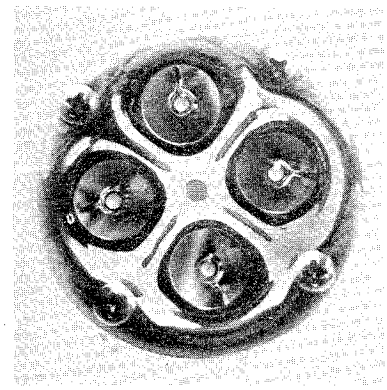

Fig. 9 Four-source array after 360-hr run.

extractor voltage, and 13 in. Hg feed pressure. Thruster temperature was held constant at 25°C throughout the entire test. After 115 hr, small variations in deflector voltage were explored to determine if the specific impulse and efficiency could be raised at constant feed pressure. The results obtained are summarized in Table 5. Based on these data, the maximum efficiency point (16.2 kv) was selected for the next long duration segment (~135 hr). For this period the specific impulse averaged 1100 sec and the efficiency 77%. There was an unexplained variation in mass flow and thrust during this period which may have been caused by foreign material in either the feed line or filter. At the end of this period, the thrust was 565 μN after being initially in the 650 μN range. Since the thrust was still well above 445 μN, the feed pressure was then lowered to 10 in. Hg in order to increase the specific impulse to an average value of 1265 sec for the remaining 100 hr of the run. This was accomplished while still maintaining 75.4% efficiency and 489 μN thrust. The thruster was in excellent operating condition at the end of the run and the test was voluntarily terminated in order to allow other experiments to proceed.

A tungsten wire neutralizer, positioned 1.25 in. downstream and 1.5 in. to the side of the exhaust, was used for the first 122 hr of the run. At this time the neutralizer filament (0.002-in. diam by 1.5-in.-long nonsag tungsten) broke. This was believed to have been caused by the combination of a small kink that was initially in the wire and by the rapid switching of the neutralizer completely off and on again for each time-of-flight experiment.

The thruster beam profile was mapped during the last 100 hr. The results, shown in Figs. 7 and 8, indicate that 90% of the beam is contained within a cone of less than a 15° half angle. However, because of an initial thruster misalignment, the beam was centered approximately 6° off the nominal symmetry axis. The post inspection test of the thruster and tank interior were especially interesting. A major portion of the tank interior was coated with dense black substance produced by backscattering from the beam. This indicates the severe environment the thruster is subjected to during testing within a 4-ft-diam by 8-ft long chamber.

The thruster received considerable backscattering because of the short collector distance (1 m) and this was quite evident from the resulting deposition pattern on the extractor (Fig. 9). The clean areas are where the extractor was kept clean by ion bombardment. The extremely black areas immediately surrounding the extractor holes are evidence that energetic bombardment in this region was minimized by the deflecting fields caused by the high positive potential in the vicinity of the emitter and deflector electrodes. Although these pictures show that there obviously was considerable backscattering to the entire thruster, the emitters themselves remained completely clean. Figure 10 is a closeup of one of the emitters. The cleanliness of the emitters was probably caused by a combination of the cleansing action of the propellant and the tendency of the thruster exhaust to molecularly pump backscattered vapor away from the thruster. Post inspection of the thruster also indicated no signs of erosion or other thruster deterioration, thus indicating that the test could have been continued for a considerably longer duration.

A final 100-hr life test was performed with a new neutralizer to further demonstrate satisfactory operation at high performance levels while being neutralized. The results are shown in Fig. 11. The final control parameters: 9 in. Hg feed pressure (~43 μg/sec mass flow), 18 kv emitter voltage, 25°C thruster temperature, 16.2 kv deflector voltage, −5 kv extractor voltage, −50 v neutralizer bias, were set in the second day of the test and the thruster was kept at these values for the remainder of the test (78 hr). The average performance over this period was 75% efficiency, 1325 sec specific impulse, 265 μa beam current, and 547 μN thrust (hence an average of 138 μN/unit). All the performance parameters remained constant to within ±3% through this period. Post inspection showed the needles to be completely clean with no traces of wear.

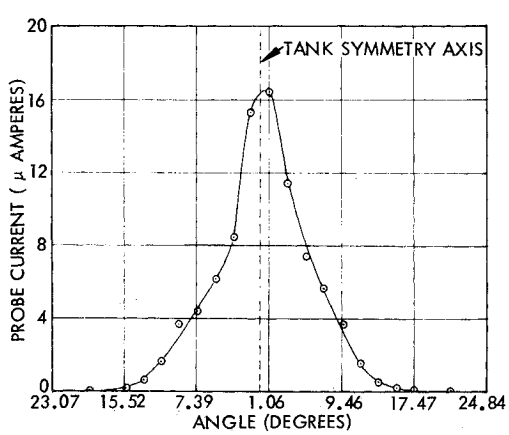

Fig. 8 East-west beam profile during last third of 360-hr test.

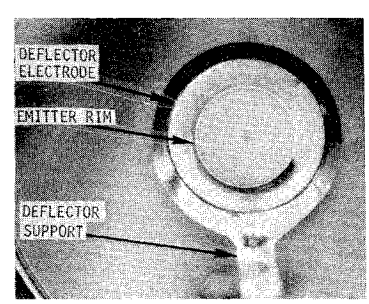

Fig. 10 Close-up of emitter and deflector electrode assembly after 360-hr test. The shaded area is due to lighting shadows when the picture was taken.

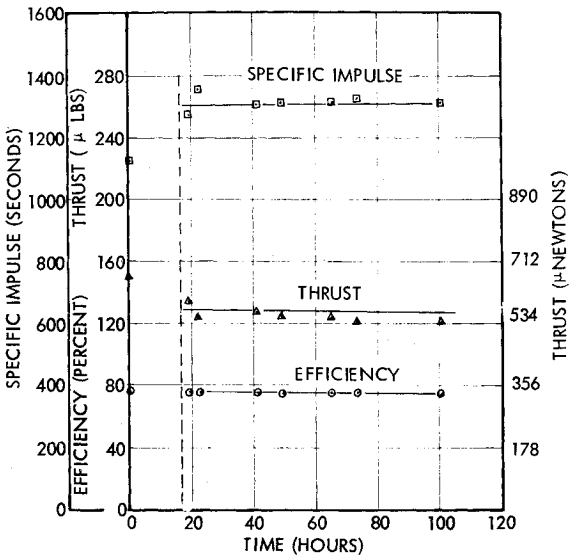

Fig. 11 Four-source array 100-hr test performance history.

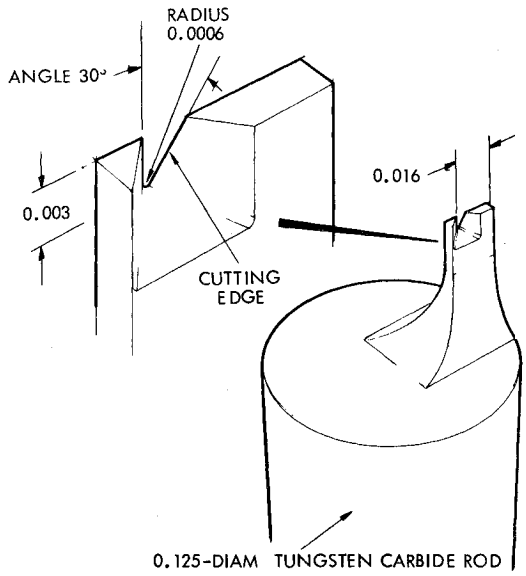

Fig. 13 Rim forming tool schematic.

Rim Forming Tool

The rim forming tool was developed to insure that uniform, reproducible emitter rims could be formed using standard jeweler's lathe techniques. The tool had a cutting edge which was essentially the negative of the cross section of the emitter rim at one point. Thus, as a rough cut emitter was rotating on a jeweler's lathe, the tool would be slowly moved forward to cut out the desired rim shape (Fig. 12).

Figure 13 is a schematic of the tool. If was formed from a length of $\frac{1}{8}$-in.-diam tungsten carbide rod. The tool was formed after first grinding off a portion of the rod's tip to leave a thin flat working section as shown in Fig. 13. The cutting groove was then formed by filing with successively thinner sheets of tungsten loaded with diamond grit. The final radius at the bottom of the groove was formed using 0.001-in. tungsten wire loaded with 1 μ diamond grit. Finally, additional material was removed from the tip of the rod as required to provide cutting clearance.

Two forming tools were used on the program. High efficiency results were obtained with the products of both tools, thus lending a fair degree of confidence to the utility of these tools.

Fig. 12 Microphotograph of lead imprint of tool formed emitter rim (scale is as shown in Fig. 13).

Conclusions

The major accomplishment of this program has been the experimental development and feasibility demonstration of tubular colloid thrusters which operate at 75% efficiency, 1300 sec specific impulse and greater than 111 μN thrust per source as measured by time-of-flight techniques. A four-source array was subjected to extensive performance testing in addition to long term runs of 100 and 360 hr. Long-term steady performance was demonstrated at several levels up to 547 μN at 75% time-of-flight efficiency and 1325 sec specific impulse. The ability to neutralize the beam without interfering with thruster performance was also demonstrated. Beam probe measurements showed that 90% of the beam was contained within a 15° half angle. The thruster's ability to provide constant performance to within $\pm$ 3% was also demonstrated. During short term testing at high-feed pressures, the four-source thruster produced 1338 μN at 70% efficiency and 1029 sec specific impulse.

References

[1] Huberman, M. N., Lear, C. W., Shelton, H., Krieve, W. F., and Kemp, R. F., "Exploratory Development of Advanced Colloid Thrusters," AFRPL-TR-71-128, Nov. 1971, Air Force Rocket Propulsion Lab., Wright-Patterson Air Force Base, Ohio.

[2] Perel, J., Mahoney, J. F., and Daley, H. L., "Colloid Thruster Technology," Final Rept. 4040, Dec. 1971, NASA Goddard Space Flight Center, Greenbelt, Md.

[3] Shelton, H. et al., "Charged Droplet Electrostatic Thruster Systems," AFAPL-TR-70-31, June 1970, Air Force Aero Propulsion Lab., Wright-Patterson Air Force Base, Ohio.

[4] Huberman, M. N. and Kidd, P. W., "Charged Particle Electrostatic Thrusters," AFAPL-TR-69-14, March 1969, Air Force Aero Propulsion Lab., Wright-Patterson Air Force Base, Ohio.

[5] Huberman, M. N. and Cohen, E., "Research on Charged Particle Electrostatic Thrusters," AFAPL-TR-67-115, Sept. 1967, Air Force Aero Propulsion Lab., Wright-Patterson Air Force Base, Ohio.